

## Research Article

### Electrostatic Separation of Biowaste: An Approach for Landfills Reduction in Malaysia

<sup>1</sup>Koonchun Lai, <sup>2</sup>Sooking Lim, <sup>1</sup>Pehchiong Teh and <sup>1</sup>Kimho Yeap

<sup>1</sup>Faculty of Engineering and Green Technologi,

<sup>2</sup>Faculty of Engineering and Science, Universiti Tunku Abdul Rahman, Malaysia

**Abstract:** Leachate and methane production due to the landfilling of biowaste has become an environmental threat. This study targets to investigate the extractability of biowaste from waste mixture as an approach of reduction of solid waste and landfill. A statistical analysis was conducted to analyze the performance of electrostatically waste separation. Individual and interactive effects of independent factors, namely rotation speed; electrical potential and electrodes interval on separation efficiency were assessed. Optimal operational conditions were deduced as 60 rpm rotation speed, 30 kV supply potential and 54 mm electrodes interval. Under these conditions, biowaste separation efficiency of 83.88% was experimentally achieved. Separation efficiency of non-biowaste was 89.51% under same operational condition. These results fitted well with the predicted model. Results in this study conclude the electrostatic separation could be an effective pre-treatment alternative in dealing with leachate and methane problems of landfilled biowaste.

**Keywords:** Analytical models, electrostatic discharge, optimization, waste recovery, waste reduction

## INTRODUCTION

Since decades, landfilling remains the most common disposal way of municipal solid waste for its simple yet cheap disposal procedure (Williams, 2005). It is about 95% of collected municipal waste was landfilled in Malaysia (Bashir *et al.*, 2010). A high amount of biowaste, particularly food waste (~45%) can be found in the solid waste, followed by plastic (~24%), paper (~7%), metal (~6%), glass (~3%) and others (~15%). Landfills in Malaysia are generally crowded and it is impractical to find new locations (Kathirvale *et al.*, 2004). Therefore, proper pre-treatment of waste, e.g., source segregation is crucial in conserving a clean environment.

Pre-treatment of waste has recently received momentous interests. To date, researchers have studied the pre-treatment of organic waste with a number of processes. These include mechanical (Lindmark *et al.*, 2012), thermo-chemical (Vavouraki *et al.*, 2014) and enzymatic (Tahezadeh and Karimi, 2008) treatments. However, very few studies were conducted using the electro-mechanical technique. This study employs electrostatic separation process to extract biowaste matter from municipal solid waste. Electrostatic separation is an environmentally friendly approach to separate two or more matters in a mixture for the difference in conductivity (Mihalescu *et al.*, 2002; Veit *et al.*, 2005).

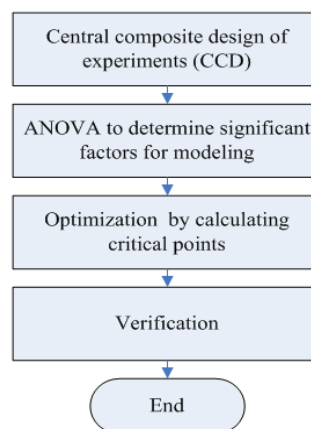


Fig. 1: Flowchart of the proposed method

In this study, a roll-type electrostatic separator has been utilized to segregate the biowaste (food) from a mixture with plastic and glass. The separator sorts the more conductive matter and less conductive matter to different locations. The food appears more conductive for its water content, making it detachable from others during the rotational separation process. However, some matter may fall between as middling product, resulting decline in separation efficiency. Main objectives of present study focus on determining the efficiency of biowaste separation by electrostatic process and building up the equations for optimal separation results with respect to operational conditions

**Corresponding Author:** Koonchun Lai, Faculty of Engineering and Green Technologi, Universiti Tunku Abdul Rahman, Malaysia

This work is licensed under a Creative Commons Attribution 4.0 International License (URL: <http://creativecommons.org/licenses/by/4.0/>).

(i.e., rotation speed, electrodes interval and supply potential). To our best knowledge, this is the first report of optimization for biowaste separation process by using electrostatic separator. The flowchart of proposed method in this study is shown in Fig. 1.

### EXPERIMENTAL PROCEDURES

An earth-grounded roller type electrostatic separator rotating in clockwise direction was employed. An ionizing needle electrode was powered by a power source (up to 35 kV) for corona discharge generation. An electrostatic plate electrode was connected beneath, providing the non-discharging electrostatic charge. The granular waste was deposited onto roller surface by a feed system. The separated and recovered products were found in the tanks under the separator. Figure 2 shows the schematic diagram of the simplified circuit to represent electrostatic separator.

The sample of test was a 100 g mixture of biowaste, BW (fruit skin) and non-biowaste, NB (glass and plastic). They were prepared respectively in portion of 40 and 60%. The granules were synthetically prepared in size within 2.0 to 4.0 mm. The granule mixture was deposited onto roller as a monolayer. Distance between the feed system and top roller position was 50.0 mm. The biowaste, non-biowaste and a portion of unsorted mixture will be collected from the tanks labelled BW and NB, respectively.

In electrostatic separation, biowaste and non-biowaste were separated by both corona and electrostatic processes due to the difference in conductivity. Surrounding air near the ionizing

electrode was ionized by a high intense corona discharge, thus forming an ionizing zone. When roller delivers the granules through the zone, the more conductive granules (biowaste) lose their charge rapidly, avoiding them from being pinned for a longer time than the less conductive one (non-biowaste). With the continuous rotation from the roller, the more conductive granules are subjected to a centrifuge force which is larger than the pinning force and thrown off the roller. The electrostatic electrode induces an evenly distributed electric field to deviate the more conductive granules from their natural falling trajectory. This improves the effectiveness and efficiency of the separation process. The less conductive granules remain pinned to the roller due to the larger pinning force applied on them. Eventually they fall off at a different location. The mass were measured by a digital precision balance with resolution of 0.01 g after each run. The separation efficiency,  $S$  (%) of biowaste,  $S_{BW}$ , non-biowaste,  $S_{NB}$  was calculated by:

$$S_{BW} = \frac{m_{BW}}{B_0} \times 100\% \quad (1)$$

$$S_{NB} = \frac{m_{NB}}{N_0} \times 100\% \quad (2)$$

where,  $m_{BW}$ ,  $B_0$ ,  $m_{NB}$  and  $N_0$  are the mass of BW tank, initial biowaste mass, mass of NB tank and initial non-biowaste mass, respectively.

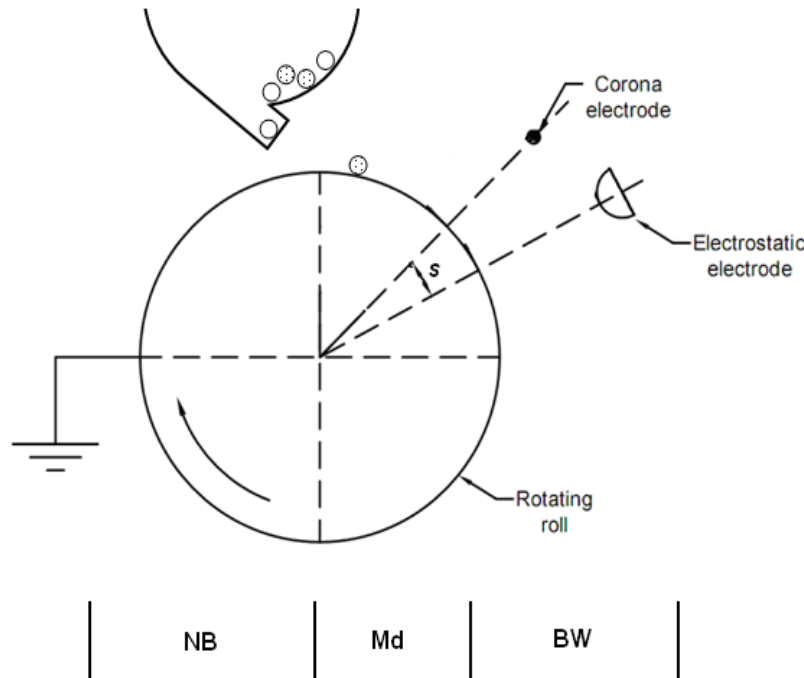


Fig. 2: Simplified circuit of the electrostatic separator design

**EXPERIMENTAL DESIGN AND ANALYSIS**

A number of factors could be analyzed simultaneously with proper design of experiments (Buang *et al.*, 2014). Besides, optimization results deduced from the statistical analysis reduce the computing effort and cost (Vlad *et al.*, 2014). During separation process, each granule would subject to several forces, e.g., centrifuge force and electrostatic force. Centrifuge force relates directly to the roller rotating speed, whereas electrostatic force relates directly to electric field strength. Thus, a Central Composite Design (CCD) was employed in the present study by considering three independent variables, namely rotation speed (*A*), electrical potential (*B*) and electrodes interval (*C*). CCD is a factorial design with a central point and  $\alpha$ -distance star topology. The three factors are tabulated in Table 1 with their levels and ranges. Value of  $\alpha$  was determined by:

$$\alpha = 2^{p/4} \tag{3}$$

and calculated as 1.68, where *p* is the number of studied factor. Separation efficiencies for biowaste and non-biowaste were chosen as response parameters. A total of 20 evaluations were performed in duplicate referring to the CCD matrix in Table 2 and the average values were used in analysis. In order to identify the critical points, the response was expressed as a quadratic model according to the following polynomial function:

$$S = \beta_0 + \sum_{i=1}^p \beta_i X_i + \sum_{i=1}^p \beta_{ii} X_i^2 + \sum_{1 \leq i < j \leq p} \beta_{ij} X_i X_j + e_i \tag{4}$$

where,

- $\beta_0$  = Constant coefficient
- $X_i, X_j$  = Independent variables
- $\beta_i, \beta_{ii}, \beta_{ij}$  = Coefficient of linear, quadratic and interaction
- $e_i$  = The error

Eq. (4) can be rewritten as:

$$S = \beta_0 + \beta_1 X_1 + \beta_2 X_2 + \beta_3 X_3 + \beta_{12} X_1 X_2 + \beta_{13} X_1 X_3 + \beta_{23} X_2 X_3 + \beta_{11} X_1^2 + \beta_{22} X_2^2 + \beta_{33} X_3^2 + e \tag{5}$$

Analysis of Variance (ANOVA) was employed to assess the fitted quality of model and statistical significance of regression coefficients. ANOVA compares the change of variable levels and the variation due to random errors of response measurement (Lee and Lee, 2012). The data dispersion (*d*) for each observation (*x*) was obtained using the equation:

Table 1: Experimental levels of independent process factors

Variable			
Levels	Factor A (rpm)	Factor B (kV)	Factor C (mm)
$-\alpha$	49.77	16.59	39.77
-1	60.00	20.00	50.00
0	75.00	25.00	65.00
1	90.00	30.00	80.00
$+\alpha$	100.23	33.41	90.23

Table 2: CCD for various experimental conditions

Run	Factor A	Factor B	Factor C	Response 1, $S_{BW}$	Response 2, $S_{NB}$
1	90.00	20.00	50.00	74.7	86.4
2	100.23	25.00	65.00	72.9	83.9
3	60.00	20.00	50.00	76.5	89.5
4	75.00	25.00	39.77	71.6	81.4
5	75.00	25.00	65.00	75.4	85.7
6	49.77	25.00	65.00	80.4	82.5
7	90.00	30.00	80.00	59.7	68.9
8	60.00	30.00	50.00	84.0	89.2
9	75.00	16.59	65.00	69.6	85.5
10	75.00	25.00	65.00	74.9	84.8
11	75.00	33.41	65.00	75.9	89.1
12	60.00	30.00	80.00	64.3	68.3
13	75.00	25.00	90.23	41.6	47.3
14	60.00	20.00	80.00	58.6	68.5
15	90.00	30.00	50.00	77.9	89.2
16	75.00	25.00	65.00	74.7	84.8
17	75.00	25.00	65.00	75.5	85.7
18	90.00	20.00	80.00	57.2	66.6
19	75.00	25.00	65.00	76.7	87.2
20	75.00	25.00	65.00	76.7	87.1

$$d = (x - \bar{x})^2 \tag{6}$$

The total sum of square ( $SS_{tot}$ ) adds all observation dispersion:

$$SS_{tot} = SS_{reg} + SS_{lf} + SS_{pe} \tag{7}$$

$$SS_{reg} = \sum_i^m \sum_j^n (x_i - \bar{x})^2 \tag{8}$$

$$SS_{lf} = \sum_i^m \sum_j^n (x_i - \bar{x}_i)^2 \tag{9}$$

$$SS_{pe} = \sum_i^m \sum_j^n (x_{ij} - \bar{x}_i)^2 \tag{10}$$

where,  $SS_{reg}$ ,  $SS_{lf}$ ,  $SS_{pe}$ , *m*, *n* and  $\bar{x}$  are the sum of error due to regression, sum of error due to loss of fit, sum of error due to pure error, number of level, number of observation and estimated value, respectively. The model quality was evaluated by values of the significance of regression test (*F*-value,  $reg$ ) and the lack of fit test (*F*-value, *lf*). A significant regression and a non-significant lack of fit imply the model could be fit well to empirical data. Values of the mentioned tests can be determined by using Eq. (11-12):

$$F_{reg} = \frac{n-k}{k-1} \cdot \frac{SS_{reg}}{SS_{lf} + SS_{pe}} \tag{11}$$

$$F_{yf} = \frac{n-m}{m-k} \cdot \frac{SS_{yf}}{SS_{pe}} \tag{12}$$

where,  $k$  is the number of parameters of the model.

Accuracy of model can be measured by coefficient of determination, or known as  $R^2$ :

$$R^2 = 1 - \frac{SS_{yf} + SS_{pe}}{SS_{tot}} \tag{13}$$

A larger value of  $R^2$  is desirable as it means high accuracy. The optimum conditions of the quadratic model can be determined by calculating the critical points. The quadratic function, Eq. (5) for three variables can be described as the first grade system in Eq. (14-16):

$$\frac{\partial S}{\partial X_1} = \beta_1 + \beta_{12}X_2 + \beta_{13}X_3 + 2\beta_{11}X_1 = 0 \tag{14}$$

$$\frac{\partial S}{\partial X_2} = \beta_2 + \beta_{12}X_1 + \beta_{23}X_3 + 2\beta_{22}X_2 = 0 \tag{15}$$

$$\frac{\partial S}{\partial X_3} = \beta_3 + \beta_{13}X_1 + \beta_{23}X_2 + 2\beta_{33}X_3 = 0 \tag{16}$$

Critical point, i.e., maximum and minimum coordinates, can be obtained by solving the system and identifying values of  $X_1$ ,  $X_2$  and  $X_3$ .

## RESULTS AND DISCUSSION

Table 2 tabulates the responses obtained under different experimental evaluation by CCD. Results reveal that separation efficiency of biowaste to be from 41.6 to 84.0% and separation efficiency of non-biowaste from 47.3 to 89.5%. Table 3 summarizes the ANOVA of regression parameters of the quadratic models for the four responses. The  $F$ -value,  $r_{reg}$  with low probability values ( $<0.0001$ ) imply the high quality of statistical significance of every model. Meanwhile, the lack of fit was non-significant relative to the pure error as the probability values were greater than 0.1000 (Korbahti and Tanyolac, 2008). The correlation coefficient ( $R^2 > 0.8000$ ) was obtained by all models, showing good agreement between the observed and deduced results (Joglekar and May, 1987).

The signal-to-noise ratio, or known as adequate precision ( $>4.00$ ) indicates an adequate signal for the model (Olmez, 2009). Based on the analysis, all models constructed in this study were considered reasonable. ANOVA results in Table 4 substantiates adequacy of the quadratic models. Significant model terms with low probability values of ( $<0.0500$ ) were selected whereas the others were excluded to improve the model. Final quadratic models were deduced for each response in Eq. (17-18) in terms of actual value of factors rotation speed ( $A$ ), electrical potential ( $B$ ) and electrodes interval ( $C$ ):

$$S_{BW} = -41.91 - 0.24A + 3.32B + 3.21C - 12.50E-003A*B + 2.39E-003A^2 - 33.67E-003B^2 - 29.11E-003C^2 \tag{17}$$

$$S_{NB} = 1.36 - 1.71B + 3.60C - 3.74E-003A^2 + 24.28E-003B^2 - 33.37E-003C^2 \tag{18}$$

To confirm if the models provide adequate approximation to the actual system, probability plots of the studentized residuals were plotted in Fig. 3 by using software of Design Expert 8.0.5. The straight line in Fig. 3 indicates residuals follow a normal distribution. The evenly scattering data at the line concludes the experimental data is normally distributed. The predicted separation efficiencies deduced from the model were plotted over the experimental data in Fig. 4. The goodness of fit between the predicted response and the empirical results is shown.

From Eq. (17), the separation efficiency of biowaste increased with a slower rotation speed, a higher electrical potential and a larger gap between electrodes. This was due to slow rotation speed prolongs the retention time of granules in ionizing zone. In addition, the high electrical potential generates a stronger electrostatic field and enhances the induction charging of conductive biowaste. With rotation speed 60 rpm, electrical potential 30 kV and electrodes interval 50 mm, the maximum separation efficiency was 83.9%. Separation efficiency of non-biowaste increased when electrodes interval was increased. Unlike biowaste separation, increment in electrical potential impaired the  $S_{NB}$  results. The rotation speed has limited effect on non-biowaste separation, with maximum separation efficiency of 89.5% with rotation speed 60 rpm, electrical potential 20 kV and electrodes interval 50 mm.

Table 3: ANOVA results for quadratic model

Response	$S_{BW}$			$S_{NB}$		
	Model	Lack of fit	Pure error	Model	Lack of fit	Pure error
SS	1885.29	4.36	3.76	2274.32	4.80	5.63
Mean square	209.48	0.87	0.75	252.7	0.96	1.13
F-value	258.17	1.16		242.32	0.85	
Prob>F	<0.0001	0.4370		<0.0001	0.5672	
$R^2$	0.9957			0.9954		
Adequate precision	65.26			58.18		

Table 4: ANOVA for significant terms

	Model	Mean square	F-value	Prob>F
$S_{BW}$	A	51.47	63.44	<0.0001
	B	63.70	78.51	<0.0001
	C	1121.41	1382.1	<0.0001
	AB	7.03	8.67	0.0147
	A <sup>2</sup>	4.16	5.12	0.0471
	B <sup>2</sup>	10.21	12.59	0.0053
$S_{NB}$	C <sup>2</sup>	618.6	762.4	<0.0001
	B	8.31	7.97	0.0181
	C	1421.86	1363.45	<0.0001
	A <sup>2</sup>	10.23	9.81	0.0106
	B <sup>2</sup>	5.31	5.09	0.0477
	C <sup>2</sup>	812.17	778.80	<0.0001

For a better understanding, the interactive relationships between responses and independent factors were represented by the three-dimensional surface response plots (Fig. 5). One factor was remained constant whereas the others were varied within the experimental ranges in each plot. In Fig. 5(a to c), the three dimensional response surface plots for biowaste separation efficiency were introduced as a function of electrical potential and electrodes interval, by keeping the rotation speed constant. Meanwhile, the combined effect of rotation speed and electrical potential on non-biowaste separation efficiency at

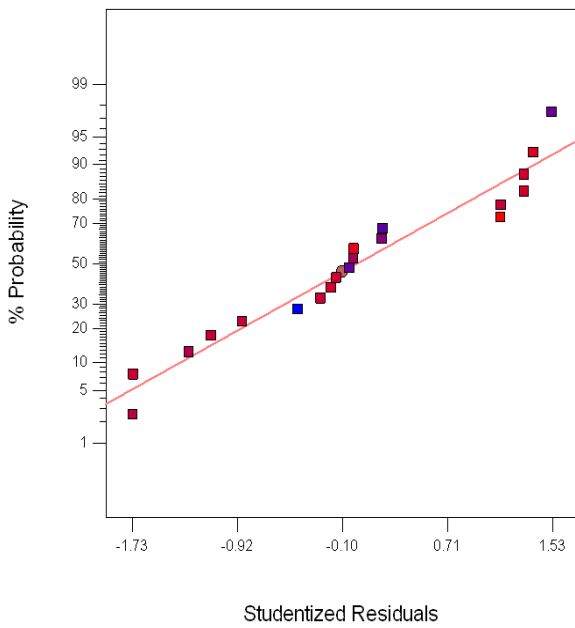


Fig. 3a: Probability plot of studentized residuals for  $S_{BW}$

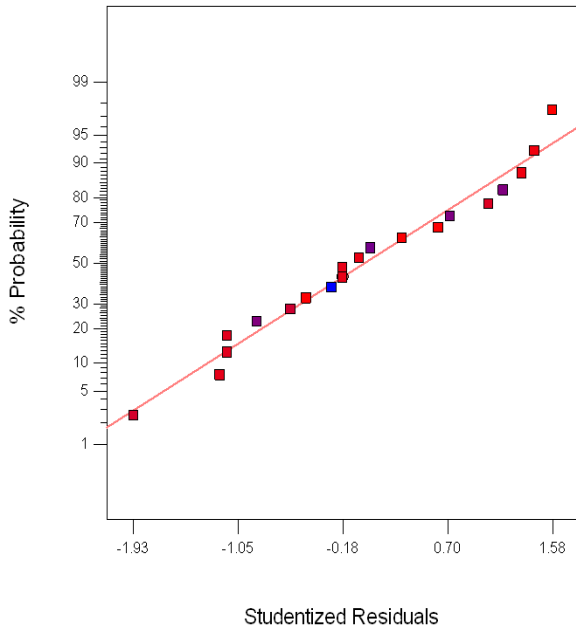


Fig. 3b: Probability plot of studentized residuals for  $S_{NB}$

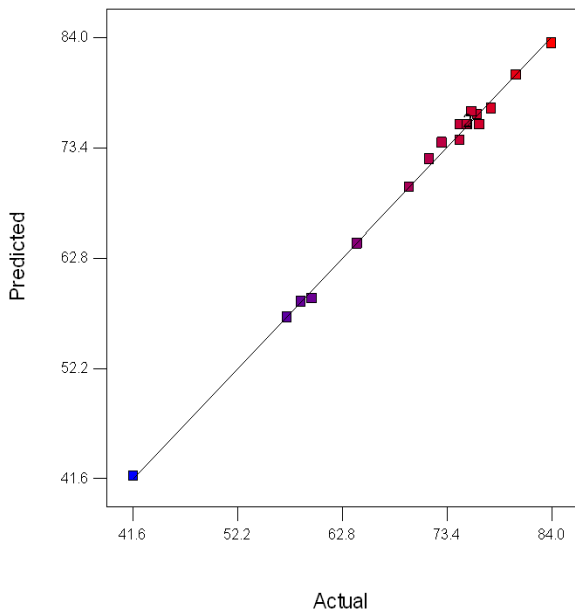


Fig. 4a: Predicted versus actual values for  $S_{BW}$

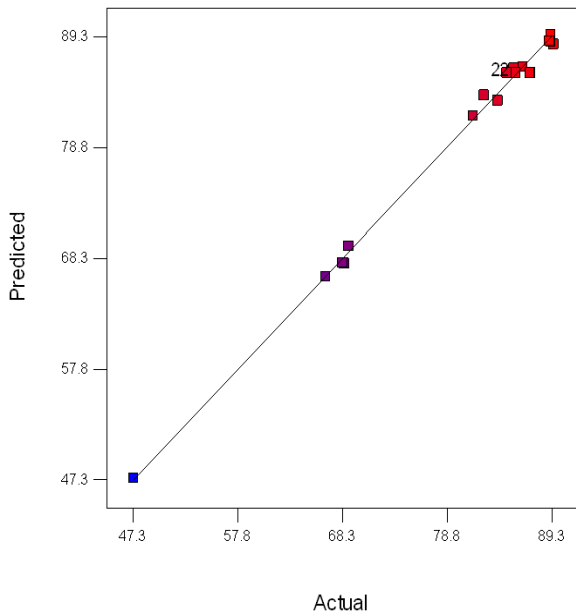


Fig. 4b: Predicted versus actual values for  $S_{NB}$

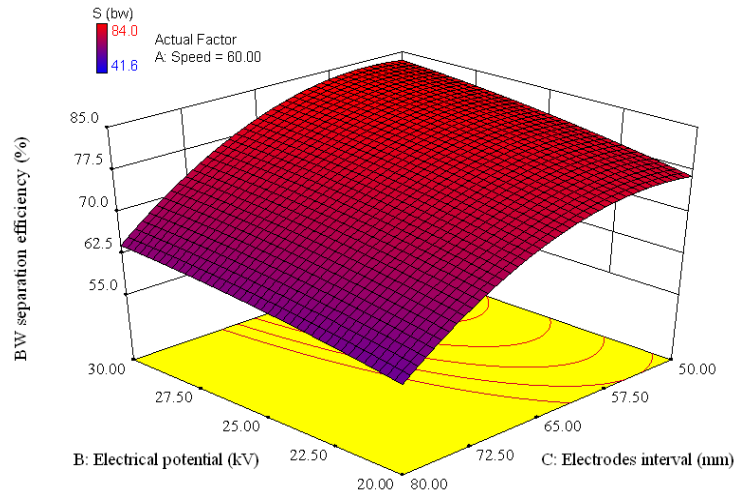


Fig. 5a: Response surface plot for biowaste separation efficiency as a function of electrical potential; kV and electrodes interval; mm (rotation speed: 60 rpm)

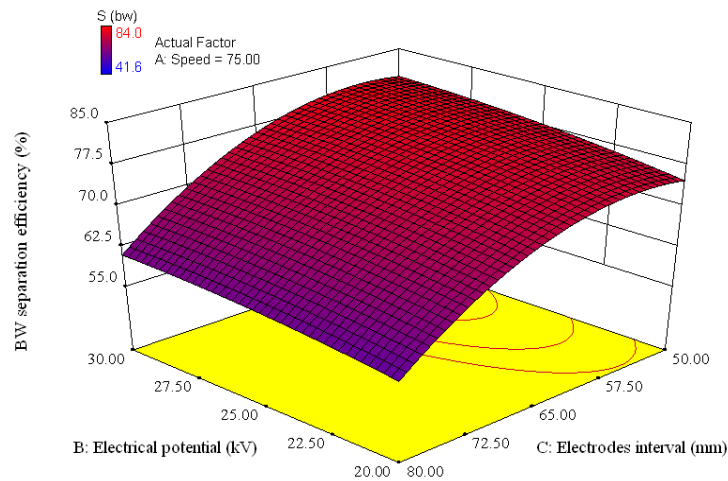


Fig. 5b: Response surface plot for biowaste separation efficiency as a function of electrical potential; kV and electrodes interval; mm (rotation speed: 75 rpm)

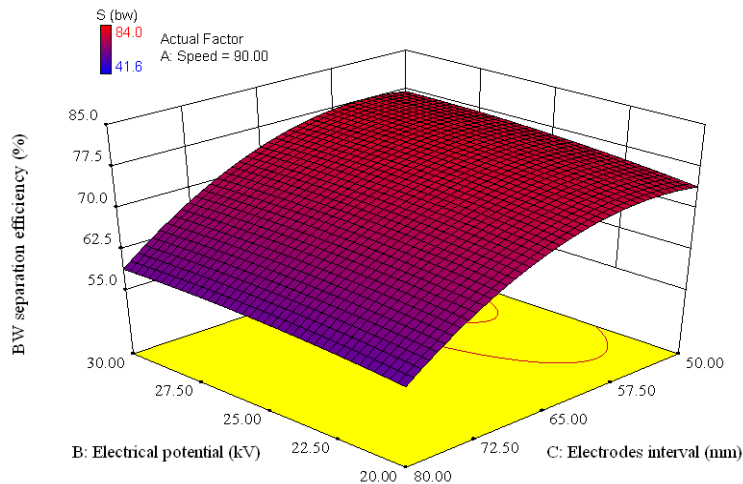


Fig. 5c: Response surface plot for biowaste separation efficiency as a function of electrical potential; kV and electrodes interval; mm (rotation speed: 90 rpm)

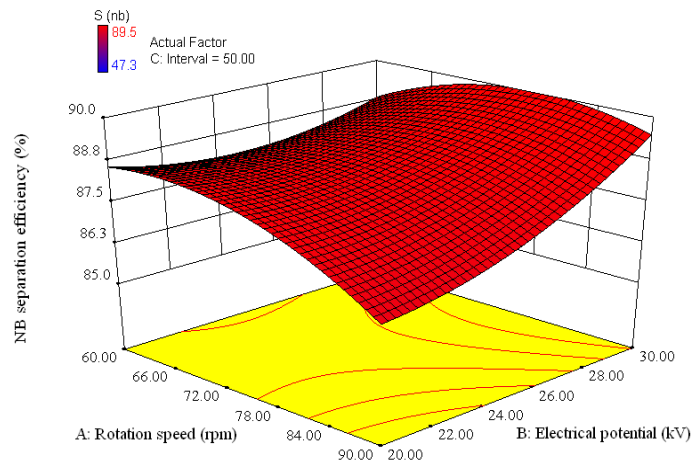


Fig. 5d: Response surface plot for non-biowaste separation efficiency as a function of rotation speed; rpm and electrical potential; kV (electrodes interval: 50 mm)

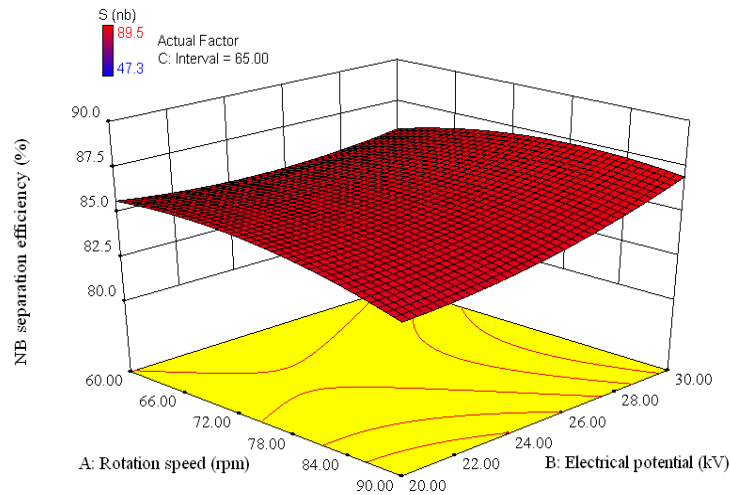


Fig. 5e: Response surface plot for non-biowaste separation efficiency as a function of rotation speed; rpm and electrical potential; kV (electrodes interval: 65 mm)

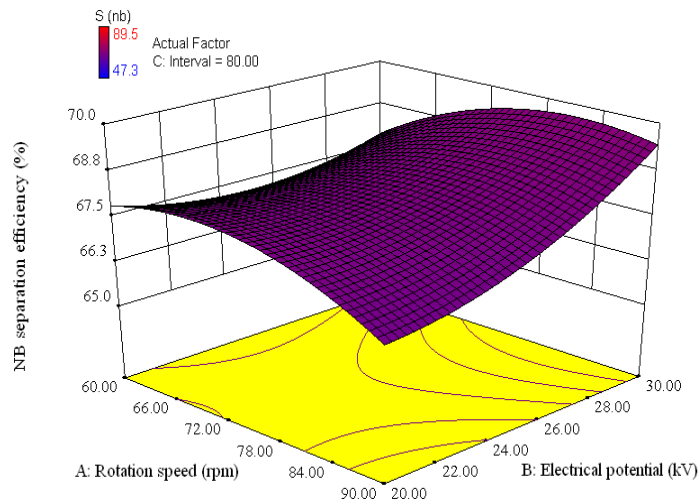


Fig. 5f: Response surface plot for non-biowaste separation efficiency as a function of rotation speed; rpm and electrical potential; kV (electrodes interval: 80 mm)

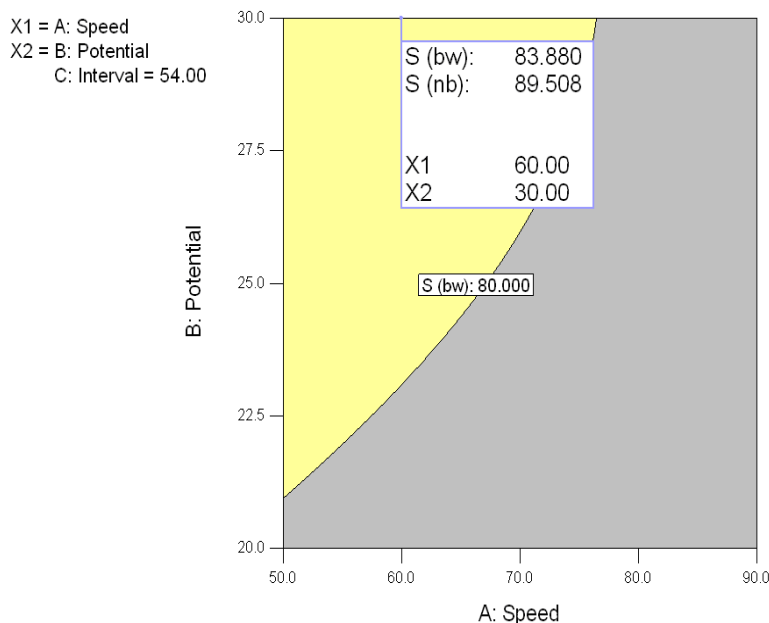


Fig. 6: Overlay plot for optimal operational conditions

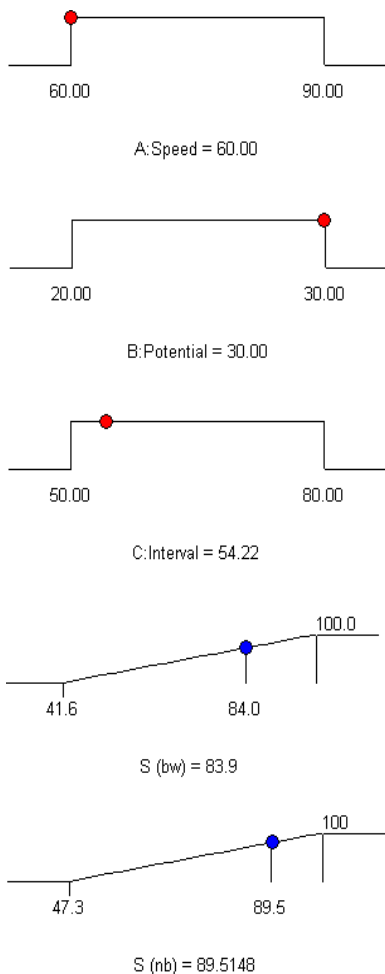


Fig. 7: Operational conditions for optimal separation efficiencies

Table 5: Comparison of experimental and statistical optimum responses

Responses	Experimental results	Statistical results
$S_{BW}$ (%)	84.20	83.88
$S_{NB}$ (%)	88.76	89.51

constant electrodes interval were showed in Fig. 5(d to f).

The overlay plot was employed to predict the optimal experimental conditions, as shown in Fig. 6. Optimal region was predicted by selecting separation efficiency higher than the arbitrarily constrained value in the plot. Apparently, maximum values of separation efficiency of biowaste and that of non-biowaste could be achieved at 83.88 and 89.51%, respectively. By referring to the model, the optimal conditions were found at rotation speed 60 rpm, electrical potential 30 kV and electrodes interval 54 mm, as illustrated in Fig. 7. Experiment under the suggested optimal conditions was performed to serve as comparison. Table 5 verifies responses obtained from laboratory experiment and model prediction were in a good agreement.

## CONCLUSION

In the present study, two responses were analyzed by using ANOVA. The maximized results of separation of both biowaste and non-biowaste were obtained with a low rotation speed (60 rpm) and high electrical potential (30 kV) within range of experiment. Electrodes interval, which played another crucial role in the models, was set at 54 mm. Prediction data fitted well with the actual data, in where experimental data was consistent with the overlay plot results. According

to the results, electrostatic separation process can be used for efficient separation and recovery of biowaste from municipal solid waste, as an approach to reduce the size of landfills and the environmental hazards.

## REFERENCES

- Bashir, M.J.K., H.A. Aziz, M.S. Yusoff, S.Q. Aziz and S. Mohajeri, 2010. Stabilized sanitary landfill leachate treatment using anionic resin: Treatment optimization by response surface methodology. *J. Hazard. Mater.*, 182: 115-122.
- Buang, F., I. Jantan, A.Z. Amran and D. Arbain, 2014. Optimization of ginger (*Zingiber officinale*) oil yield from Malaysia in different hydrodistillation physical parameters via central composite design of response surface methodology (RSM). *Res. J. Appl. Sci. Eng. Technol.*, 7(24): 5098-5105.
- Joglekar, A.M. and A.T. May, 1987. Product excellence through design of experiment. *Cereal Food World*, 32: 857-868.
- Kathirvale, S., M.N. Muhd Yunus, K. Sopian and A.H. Samsuddin, 2004. Energy potential from Municipal Solid Waste in Malaysia. *Renew. Energ.*, 29(4): 559-567.
- Korbahti, B.K. and A. Tanyolac, 2008. Electrochemical treatment of simulated textile wastewater with industrial components and Levafix Blue CA reactive dye: Optimization through response surface methodology. *J. Hazard. Mater.*, 151: 422-431.
- Lee, C.Y. and Z.J. Lee, 2012. A novel algorithm applied to classify unbalanced data. *Appl. Soft Comput.*, 12: 2481-2485.
- Lindmark, J., N. Leksell, A. Schnürer and E. Thorin, 2012. Effects of mechanical pre-treatment on the biogas yield from ley crop silage. *Appl. Energ.*, 97: 498-502.
- Mihailescu, M., A. Samuila, A. Urs, R. Morar, A. Iuga and L. Dascalescu, 2002. Computer-assisted experimental design for the optimisation of electrostatic separation processes. *IEEE T. Ind. Appl.*, 38: 1174-1181.
- Olmez, T., 2009. The optimization of Cr(VI) reduction and removal by electrocoagulation using response surface methodology. *J. Hazard. Mater.*, 162: 1371-1378.
- Taherzadeh, M.J. and K. Karimi, 2008. Pretreatment of lignocellulosic wastes to improve ethanol and biogas production: A review. *Int. J. Mol. Sci.*, 9: 1621-1651.
- Vavouraki, A.I., V. Volioti and M.E. Kornaros, 2014. Optimization of thermo-chemical pretreatment and enzymatic hydrolysis of kitchen wastes. *Waste Manage.*, 34: 167-173.
- Veit, H.M., T.R. Diehl, A.P. Salami, J.S. Rodrigues, A.M. Bernardes and J.A.S. Tenorio, 2005. Utilization of magnetic and electrostatic separation in the recycling of printed circuit boards scrap. *Waste Manage.*, 25: 67-74.
- Vlad, I., A. Campeanu, S. Enache and G. Petropol, 2014. Operation characteristics optimization of low power three-phase asynchronous motors. *Adv. Electr. Comp. Eng.*, 14: 87-92.
- Williams, P.T., 2005. *Waste Treatment and Disposal*. 2nd Edn., John Wiley and Sons Ltd., England.